

CrystEngComm

Accepted Manuscript



This is an *Accepted Manuscript*, which has been through the Royal Society of Chemistry peer review process and has been accepted for publication.

Accepted Manuscripts are published online shortly after acceptance, before technical editing, formatting and proof reading. Using this free service, authors can make their results available to the community, in citable form, before we publish the edited article. We will replace this *Accepted Manuscript* with the edited and formatted *Advance Article* as soon as it is available.

You can find more information about *Accepted Manuscripts* in the [Information for Authors](#).

Please note that technical editing may introduce minor changes to the text and/or graphics, which may alter content. The journal's standard [Terms & Conditions](#) and the [Ethical guidelines](#) still apply. In no event shall the Royal Society of Chemistry be held responsible for any errors or omissions in this *Accepted Manuscript* or any consequences arising from the use of any information it contains.

Larger pores and higher T_c : $\{[\text{Ni}(\text{cyclam})]_3[\text{W}(\text{CN})_8]_2 \cdot \text{solv}\}_n$ - a new member of the largest family of pseudo-polymorphic isomers among octacyanomethylate-based assemblies

Beata Nowicka,^{*a} Mateusz Reczyński,^a Michał Rams,^b Wojciech Nitek,^a Marcin Koziel^a and Barbara Sieklucka^a

^a*Faculty of Chemistry, Jagiellonian University, Ingardena 3, 30-060 Kraków, Poland*

^b*Institute of Physics, Jagiellonian University, Łojasiewicza 11, 30-348 Kraków, Poland*

Abstract

A new crystalline pseudo-polymorphic form of the 2-D microporous honeycomb-like magnetic network $\{[\text{Ni}(\text{cyclam})]_3[\text{W}(\text{CN})_8]_2 \cdot \text{solv}\}_n$ was obtained in the reaction between methanol-soluble $\{\text{Ni}[\text{Ni}(\text{MeOH})_3]_8[\text{W}(\text{CN})_8]_6\}$ clusters and the $[\text{Ni}(\text{cyclam})]^{2+}$ complex in acetonitrile-rich solvent mixture. In comparison to the three earlier characterised pseudo-polymorphs, which all crystallised in the triclinic space group P-1, the new form shows higher symmetry of C2/m, greater porosity of ca. 40% solvent accessible volume, and the highest magnetic ordering temperature of 12 K. It undergoes an irreversible single-crystal-to-single-crystal transformation to the hexadecahydrate form that is stable in air at ambient temperature. A new synthetic pathway leading directly to methanol solvate of the same network, which was previously obtained by sorption of MeOH into the anhydrous form, is also reported.

Keywords

Porosity; Molecular magnetism; Structural dynamics; Octacyanotungstate; Nickel cyclam.

Introduction

Molecular magnetic materials that show porosity and the ability to absorb guest molecules attract growing attention due to their potential applications in the construction of chemosensitive switches as well as gas storage and the neutralisation of harmful substances.¹ The study of open framework structural transformations upon guest sorption and the resulting changes in magnetic properties is important for the understanding of magneto-structural correlations in coordination polymers.² Furthermore, compounds characterised by network dynamics restricted to changes in bond lengths and angles give unique opportunity to establish the influence of this particular factor on magnetic properties.

We have earlier characterised two structurally dynamic networks based on Ni-cyclam complex and octacyanometallates: $\{[\text{Ni}(\text{cyclam})]_3[\text{W}(\text{CN})_8]_2\}_n$ (**1**)^{3,4} and $\{[\text{Ni}(\text{cyclam})]_2[\text{Nb}(\text{CN})_8]\}_n$,⁵ both of which show long-range magnetic ordering. The magnetic changes accompanying dehydration of Ni-Nb(IV) network proved to be only partially reversible. Conversely, the Ni-W(V) network shows a rare phenomenon of fully reversible single-crystal-to-single-crystal transformation upon dehydration. Its 2D structure consists of honeycomb-like layers intersected by channels of 0.5 nm in diameter, which places it in the class of microporous materials. In our previous studies^{3,4} we described three forms of this network: anhydrous $\{[\text{Ni}(\text{cyclam})]_3[\text{W}(\text{CN})_8]_2\}_n$ (**1**), hydrated $\{[\text{Ni}(\text{cyclam})]_3[\text{W}(\text{CN})_8]_2 \cdot 16\text{H}_2\text{O}\}_n$ (**1h**) and methanol-modified $\{[\text{Ni}(\text{cyclam})]_3[\text{W}(\text{CN})_8]_2 \cdot n\text{MeOH}\}_n$ (**1m**). In this paper we present a new $\{[\text{Ni}(\text{cyclam})]_3[\text{W}(\text{CN})_8]_2 \cdot \text{solv}\}_n$ (**1c**) (solv = $n\text{H}_2\text{O} \cdot m\text{MeOH} \cdot k\text{MeCN}$) form, which differs in structure and magnetic properties from the others. Here we also describe a new synthetic pathway leading directly to the methanol-modified form **1m**, which was earlier obtained through immersion of anhydrous compound **1** in MeOH.⁴

Compound **1c** is obtained in the reaction between $\{\text{Ni}[\text{Ni}(\text{MeOH})_3]_8[\text{W}(\text{CN})_8]_6\}$ clusters and $[\text{Ni}(\text{cyclam})]^{2+}$. Nickel(II) combined with octacyanometallates(V) in methanol forms stable and well soluble pentadecanuclear Ni_9M_6 clusters.⁶ The addition of blocking ligands leads to insoluble surface-modified clusters.⁷ Similar clusters based on Mn(II) and Co(II)⁸ have been successfully organised into extended structures by replacing labile MeOH coordinated to outer metal ions with organic bridging ligands.⁹ We attempted to link pentadecanuclear clusters by the $[\text{Ni}(\text{cyclam})]^{2+}$ complex using terminal CN groups present on its surface. However, under slow diffusion conditions the reaction led to the decomposition of clusters and resulted in the formation **1c**.

Experimental

Synthesis

$[\text{Ni}(\text{cyclam})(\text{NO}_3)_2]^{10}$ and $(\text{TBA})_3[\text{W}(\text{CN})_8]$ (TBA = tetrabutylammonium ion)¹¹ were synthesised according to the published methods. Other reagents and solvents of analytical grade were used as supplied.

$\{[\text{Ni}(\text{cyclam})]_3[\text{W}(\text{CN})_8]_2 \cdot \text{solv}\}_n$ (**1c**): The methanolic solutions of $(\text{TBA})_3[\text{W}(\text{CN})_8]$ (0.067 mmol, 75.0 mg; 10 ml) and $\text{Ni}(\text{NO}_3)_2 \cdot 6\text{H}_2\text{O}$ (0.100 mmol, 29.0 mg; 10 ml) were mixed together. The solution immediately turned yellow upon the formation of $\{\text{Ni}[\text{Ni}(\text{MeOH})_3]_8[\text{W}(\text{CN})_8]_6\}$ cluster. Then acetonitrile (10 ml) and water (10 ml) were added and the solution was layered upon the solution containing $[\text{Ni}(\text{cyclam})](\text{NO}_3)_2$ (0.100 mmol, 38.3 mg) in a mixture of water (26 ml), methanol (6 ml), ethanol (3 ml) and acetonitrile (2 ml) with buffer layer composed of water, acetonitrile and methanol (v:v 5:4:1). After one week brown block-shaped crystals were collected, washed several times by decantation with a mixture of solvents analogical to the mother liquor and kept under it. For elemental analysis and IR the crystals were removed from the solvent and dried in air resulting in the hydrated form $\{[\text{Ni}(\text{cyclam})]_3[\text{W}(\text{CN})_8]_2 \cdot 16\text{H}_2\text{O}\}_n$ (**1h**). Found: C 29.66; H 5.57; N 21.12. Calc. for $\text{C}_{46}\text{H}_{104}\text{N}_{28}\text{O}_{16}\text{Ni}_3\text{W}_2$: C 29.88; H 5.67; N 21.21. IR (νCN): 2109, 2139, 2161, 2177 cm^{-1} .

$\{[\text{Ni}(\text{cyclam})]_3[\text{W}(\text{CN})_8]_2 \cdot n\text{MeOH}\}_n$ (**1m**): $(\text{TBA})_3[\text{W}(\text{CN})_8]$ (0.067 mmol, 75.0 mg) was dissolved in methanol (10 ml) and acetonitrile (1 ml) mixture. The solution was layered upon the solution of $[\text{Ni}(\text{cyclam})](\text{NO}_3)_2$ (0.100 mmol, 38.3 mg) in a water/methanol mixture (v:v 1:1; 15 ml) with the addition of acetonitrile (1 ml). The buffer layer was composed of methanol, water and acetonitrile (v:v 2:1:0.2). After one week thin, brown slab-shaped crystals were collected and washed with a mixture of solvents analogical to the mother liquor. For elemental analysis and IR the crystals were removed from the solvent and dried in air resulting in **1h**. Found: C 29.49; H 5.24; N 21.35. Calc. for $\text{C}_{46}\text{H}_{104}\text{N}_{28}\text{O}_{16}\text{Ni}_3\text{W}_2$: C 29.88; H 5.67; N 21.21. IR (νCN): 2111, 2141, 2162, 2176 cm^{-1} .

Structure determination

Diffraction data for compound **1c** were collected on a single crystal sealed in a capillary under solvent mixture analogical to the mother liquor at room temperature using the Oxford Diffraction SuperNova four circle diffractometer equipped with the Mo (0.71069 Å) $K\alpha$ radiation source and graphite monochromator. The structure was solved by direct methods using SIR-97¹² in space group C2 suggested by CrysAlisPro¹³ diffraction data processing software. The ADDSYMM procedure of PLATON¹⁴ pointed to higher symmetry (C2/m) and the refinement and further calculations were carried out in the space group C2/m using

SHELXL-97.¹⁵ The possibility of twinning was tested and ruled out by TWINROTMAP procedure. The 1,4,8,11-tetraazacyclotetradecane ligand on Ni4 suffers strong disorder. Nitrogen atoms N31 and N32 connected to Ni4 were located from the difference Fourier map. To fulfill the symmetry requirements the two- and three-carbon fragments of the macrocycle were considered to be located at the same position with 50% probability. Three carbon atoms (C34, C35 and C37) found from the difference Fourier map were given partial occupancy values of 5/6 to add up to ten carbon atoms for the whole ring. Solvent molecules were refined isotropically. The rest of the non-hydrogen atoms were refined anisotropically using weighted full-matrix least-squares on F^2 . All hydrogen atoms joined to carbon atoms were positioned with an idealized geometry and refined using a riding model with $U_{\text{iso}}(\text{H})$ fixed at 1.2 U_{eq} of C and 1.5 U_{eq} for methyl groups. For solvent and highly disordered cyclam ring H atoms were not considered, but included in the formula. After the refinement of all atoms there was still some residual electron density in the cavities of the structure indicating the presence of additional disordered water molecules. Therefore, the data were corrected for disordered solvent using the SQUEEZE option in Platon.¹⁴ Graphics were created by Mercury 3.3.¹⁶

1c: $\text{C}_{48}\text{H}_{96}\text{N}_{28}\text{Ni}_3\text{W}_2\text{O}_{10}$; $M_r = 1769.35$; monoclinic $C2/m$, $a = 32.105(5)$, $b = 15.068(5)$, $c = 9.331(5)$ Å; $\beta = 90.772(5)^\circ$; $V = 4514(3)$ Å³; $T = 293(2)$; $Z = 2$; $D_c = 1.302$ g cm⁻³; $\mu(\text{Mo K}\alpha) = 3.208$ mm⁻¹; $F(000) = 1784$; 31680 reflections collected, of which 5594 are unique ($R_{\text{int}} = 0.0343$); $\text{GOF} = 1.102$; $R_1 = 0.0307$ and $wR_2 = 0.0866$ [$I > 2\sigma(I)$].

Measurements

Elemental analyses were performed on an ELEMENTAR Vario Micro Cube CHNS analyzer. Magnetic measurements were performed using a Quantum Design MPMS-XL equipped with a 5 T magnet. Polycrystalline samples of **1c** and **1m** were immersed in the mixture of solvents analogous to the mother liquor and sealed in a glass tube. The samples were weighted after magnetic measurements, and after drying in air. Thus, the molecular weight of **1h** - the form stable at ambient conditions was used in all cases to scale the magnetic data. Sample **1h** was inserted in the magnetometer at 200 K to avoid the loss of crystallization solvent under vacuum. The diamagnetic correction for sample holders and solvents was estimated and subtracted. Powder XRD patterns of **1c** and **1m** in the form of thick suspensions sealed in 0.7 mm glass capillaries were measured on a PANalytical X'Pert PRO MPD diffractometer with a capillary spinning add-on using $\text{CuK}\alpha$ radiation ($\lambda = 1.54187$ Å). The patterns were collected at room temperature between 3 and 70° 2 θ angle. The reference powder patterns were generated using Mercury 3.3 software.¹⁴

Discussion

Synthetic pathways and structural transformations

The 2D honeycomb-like network was first obtained as a hydrated form $\{[\text{Ni}(\text{cyclam})]_3[\text{W}(\text{CN})_8]_2 \cdot 16\text{H}_2\text{O}\}_n$ (**1h**), which is stable in air at ambient conditions.³ We have subsequently characterised two more forms of this network differing in structure and magnetic properties: anhydrous **1a**,³ obtained by heating **1h** above 40°C, and methanol-modified **1m**,⁴ obtained by the sorption of MeOH into **1a**. In this work we present a new member of the family of pseudopolymorphs of **1**: $\{[\text{Ni}(\text{cyclam})]_3[\text{W}(\text{CN})_8]_2 \cdot \text{solv}\}_n$ (**1c**) obtained in the reaction between $[\text{Ni}(\text{cyclam})]^{2+}$ and $\{\text{Ni}[\text{Ni}(\text{MeOH})_3]_8[\text{W}(\text{CN})_8]_6\}$ clusters in the acetonitrile-methanol-water solution, as well as newly discovered synthetic pathway leading directly to **1m**.

Figure 1 shows the synthetic routes and inter-conversion pathways between four pseudopolymorphic forms of **1**. Hydrate **1h** is obtained in the reaction between $[\text{Ni}(\text{cyclam})]^{2+}$ and $[\text{W}(\text{CN})_8]^{3-}$ in water-ethanol solution. Heated above 40°C it loses crystallisation water retaining its crystalline form to give anhydrous **1a**, which differs in structure and magnetic properties from **1h**. **1a** can absorb moisture from air and reproduce **1h** in a fully reversible single-crystal-to-single-crystal transformation. It can also be modified by the sorption of methanol to give **1m**. This transformation causes loss of the monocrystalline form and was found to introduce even more pronounced changes in structure and magnetic properties.⁴ **1m** can re-enter form **1a** by drying at 40°C. In humid atmosphere at ambient temperature MeOH is exchanged directly into water to form **1h**.

In this work we present a new pseudopolymorph of the network $\{[\text{Ni}(\text{cyclam})]_3[\text{W}(\text{CN})_8]_2 \cdot \text{solv}\}_n$ (**1c**), which we denoted as a cluster-originated form. **1c** is obtained by slow diffusion of $\{\text{Ni}[\text{Ni}(\text{MeOH})_3]_8[\text{W}(\text{CN})_8]_6\}$ clusters, formed *in situ* in MeOH,⁶ into acetonitrile-methanol-water solution of $[\text{Ni}(\text{cyclam})](\text{NO}_3)_2$ in the form of block-shaped brown crystals after one week. Form **1c** can also be obtained in the reaction of $[\text{Ni}(\text{cyclam})]^{2+}$ and $[\text{W}(\text{CN})_8]^{3-}$ from the same solvent mixture, which proves that the presence of cluster is not a necessary condition of its formation. However, we observed that gradual decomposition of the clusters resulting in slow release of the $[\text{W}(\text{CN})_8]^{3-}$ ions facilitates the growth of good quality crystals. The crystals of **1c** are stable for several weeks if kept under the mixture of solvents analogical to the mother liquor. When removed from solvents and left in air they undergo transformation to the hydrated form **1h**, surprisingly with the retention of crystallinity. The transformation was confirmed by subsequent single crystal XRD measurements, as well as powder XRD and magnetic measurements on a bulk sample (Figs.

S1-S3) The hydrated form obtained in that manner enters the cycle of transformations presented in Fig.1 in same way as the sample obtained directly as **1h** from the synthesis. However, the original form of **1c** cannot be re-entered neither by an exchange of solvent guest molecules in **1h**, nor by sorption of appropriate solvent mixture by anhydrous **1a**.

We have also found a new synthetic route leading directly to the crystalline methanol solvate $\{[\text{Ni}(\text{cyclam})]_3[\text{W}(\text{CN})_8]_2 \cdot n\text{MeOH}\}_n$ **1m**, obtained earlier as powder by MeOH sorption into anhydrous sample **1a**.⁴ The crystals of **1m** grew from a methanol rich solution. Unfortunately they were too small for X-ray diffraction studies and only the elemental cell dimensions could be established from single-crystal measurements, while the structure was confirmed by PXRD. Contrary to **1c**, the crystals of **1m** collapsed when removed from the solvent, which shows that the pathway from **1m** to **1h** is also connected with the loss of the monocrystalline form.

The four presented forms of **1** constitute the largest family of pseudo-polymorphic supramolecular isomers¹⁷ among octacyanometallate-based assemblies.¹⁸ It is noteworthy that all solvates can be obtained in crystalline form directly from the synthesis in appropriate solvent media and two of them can be reproduced by sorption of solvent molecules into the de-solvated form.

Structure comparison

The structure of **1c** (Fig. S4) presents the same 2D topology as earlier characterised forms (Fig. 2): hydrated $\{[\text{Ni}(\text{cyclam})]_3[\text{W}(\text{CN})_8]_2 \cdot 16\text{H}_2\text{O}\}_n$ (**1h**), anhydrous $\{[\text{Ni}(\text{cyclam})]_3[\text{W}(\text{CN})_8]_2\}_n$ (**1a**)³ and MeOH-modified $\{[\text{Ni}(\text{cyclam})]_3[\text{W}(\text{CN})_8]_2 \cdot n\text{MeOH}\}_n$ (**1m**).⁴ Ni ion has equatorially coordinated cyclam ligand and two CN bridges in axial positions. Each octacyanotungstate is located at the node of the honeycomb-like layer and forms three CN-bridges to neighbouring Ni ions. However, in contrast to other forms which were all triclinic, **1c** shows higher symmetry in monoclinic system. All metal centres occupy special positions: W1 lies on a mirror plane, Ni2 on an inversion centre and Ni4 at a site with 2/m symmetry. Therefore the asymmetric unit consists of one-half W1, one-half Ni2 and a quarter Ni4 ions. This implies that two Ni ions, which in the structures **1h**, **1a** and **1m** are denoted Ni2 and Ni3, in **1c** are symmetry related and denoted Ni2. W1 and Ni4, together with the C16-N16 bridge connecting them lay within the mirror plane. The cyclam ligand coordinated to Ni4 is heavily disordered. The nitrogen atoms N31 and N32 show high values of thermal displacement parameters and elongation of the ellipsoids within the ring plane. Due to symmetry requirements all four fragments of the chain between N31 and N32 must be

identical, which means that the position of two- and three- carbon sections of the macrocycle in the structure are interchangeable. It suggests that the cyclam ring can either freely rotate around the central atom or adopts random positions.

The channels that run along *c* axis (corresponding to *a* axis in **1a**, **1h** and **1m**) are filled with crystallisation solvent, which probably includes water, methanol and acetonitrile used in synthesis. However, due to high disorder, only 2 MeOH and 8 H₂O molecules (split into partially occupied positions) per formula unit could be localised in the structure, and the exact amount of each solvent could not be established. The channels are approximately round in shape and are significantly larger than in the other forms of **1**. The channel diameter calculated taking into account van der Waals radii is ca. 0.8 nm for **1c** as compared to 0.5 nm for **1a**. The enlargement of the channels is reflected in the increase of volume per formula unit in the series **1a-1h-1m-1c** (Table 1). In this respect the difference between hydrated **1h** and anhydrous **1a** is relatively small (2.5%), and the transition between them is fully reversible and undergoes with the retention of crystalline form. The transformation of **1a** into **1m** is accompanied by a 12.5% increase in volume. Interestingly, **1c** has even larger volume - 18% higher than **1a**. It is surprising that despite the large difference in cell volume, the transformation from **1c** to **1h** can be achieved with the retention of crystallinity. The solvent accessible void in **1c** could not be accurately calculated due to the disorder of one of the cyclam rings, but it can be roughly estimated from the increase in cell volume at about 40% as compared to 27% and 30% for **1a** and **1h**, respectively.

There are several factors governing the amount of void space and channel size in the structure of **1**. The most important from the point of view of magnetic properties is the straightening of cyano bridges. As we discussed earlier^{3,4} Ni-N-C angles strongly influence the nature and strength of magnetic exchange between the metal centres. In **1c** the angle values are much higher than in **1a** or **1h** and approach 180°. Also, the Ni-W distances, which we consider indicative for bridge angles in **1m**, in **1c** are the longest among all forms. However, the difference between the MeOH-modified phase **1m** and **1c**, which was obtained from MeOH-rich solution, is not substantial, much smaller than the changes caused by solvent sorption upon **1a** → **1h** or **1a** → **1m** transitions. The second important aspect of the structure is the distance between honeycomb-like layers. It does not change upon water sorption, but increases by 9% if methanol is absorbed. In **1c** the distance is only slightly longer than in **1m**. This structural feature seems to be controlled by hydrogen bonding: by forming hydrogen bonds to terminal CN ligands water binds the layers together, while larger MeOH molecules push them apart squeezing between aliphatic parts of cyclam.

The two factors discussed above show similarity between MeOH-modified **1m** and cluster-originated **1c** and do not explain the striking difference in volume and channel dimensions between these two forms. Therefore, we looked more closely at the aspects of the structure which we had not discussed in detail for the earlier characterised forms. First we considered the geometry of $[\text{W}(\text{CN})_8]^{3-}$ ion as a three-connected node of the network. The SHAPE parameters¹⁹ indicate that of two most prevalent eight-coordinated geometries, in **1a**, **1h** and **1m** the W(V) environment is closer to a dodecahedron (TDD-8), while in **1c** it is almost an ideal square antiprism (SAPR-8). It has important implications for the shape of the network. Of the three angles between the bridges at the W node one is close to 90° and two others are close or higher than 120°. As the nodes do not lay in one plane the angles add up to less than 360°, but the sum increases in the series **1a** < **1h** < **1m** < **1c**, indicating the flattening of the corrugated layers. If we calculate the thickness of the layer defined by metal centres, disregarding all terminal ligands, as presented in bottom part of Fig. 2, the decrease is considerable (Table 1). Together with increasing W-Ni distances the layer flattening results in the growing size of the hexagonal ring, as can be seen in top part of Fig. 2. The figure also depicts the deformation of the honeycomb. In **1a** and **1c** the hexagon is elongated in the direction of vertices, while in **1h** and **1m** it is elongated in the direction of the edges. The ring size, defined as an average distance between opposite metal centres increases in the series **1a** < **1h** < **1m** < **1c**. Moreover, the relative position of the layers varies between pseudopolymorphs: the ring openings are not placed directly above each other, but are slid to a different degree, causing the channels to cross the layers at different angle (Table 1). It increases by nearly 7° in the series **1a** < **1h** < **1c** \approx **1m**. Combined with an expanding ring size it results in an increased channel diameter.

Magnetic properties

The magnetic susceptibility of **1c** measured at 1 kOe is presented in Figure 3 as the χT product. It reaches 4.8 cm³K/mol at 150 K, close to 4.4 cm³K/mol expected for a Ni₃W₂ unit with $s = 1$, $g = 2.2$ for Ni^{II} and $s = 1/2$, $g = 2.0$ for W^V. At lower temperatures χT increases, which suggests that some ferromagnetic interactions are predominant²⁰. A sharp maximum observed on $\chi(T)$ around 12 K points to an antiferromagnetic ordering transition. The isothermal magnetization measured at 2 K (Fig. 4) confirms the AF state, since dM/dH has a maximum around $H_{sf} = 3.2$ kOe, indicating a metamagnetic transition. The magnetization increases to $M_s = 8.0$ N β at 50 kOe, which is close to the expected saturation value of 8.6 N β .

The open hysteresis loop (Fig. 4 inset) has the remnant magnetisation of $0.25 N\beta$ and the coercive field of 650 Oe. Zero-field cooling and field cooling curves at low field (Fig. 3 inset) diverge below the maximum at 12.0 K. Both the zfc/fc bifurcation and the hysteresis loop point to an irreversibility of the magnetization process and a small ferromagnetic-like signal in **1c**. Additional susceptibility measurements with small temperature spacing around the $\chi(T)$ maximum using different fields are shown in Figure 5. They reveal a sharp spike at 12.2 K present only at low field applied. At 10 Oe the width of the peak at half height is below 0.2 K, which is the reason why it was not registered in the zfc/fc measurement. The spike at 12.2 K on the top of the usual AF peak allows us to clearly identify the origin of the observed irreversibility as a small canting of the antiferromagnetic structure leading to an uncompensated magnetization, known as weak-ferromagnetism. This mechanism was first explained by Moriya²¹ and observed in numerous inorganic (e.g. NiF₂) and molecular compounds.²² In such a model also the characteristic spike may appear in susceptibility close to T_N .

The crystal structure of **1c** suggests that intra-layer magnetic interactions through superexchange between Ni and W in -CN- bridges₇ are much stronger than any inter-layer interactions. They are responsible for the Curie-Weiss temperature $\theta_{CW} = 13.0(5)$ K determined from the susceptibility data in the 50-150 K range. From the relation $2z|J|k_B M_s = H_s g^2 \beta$, we estimate the inter-layer interaction constant to be $J' = 0.03$ K per Ni₃W₂ unit.

Magnetic data for **1a**, **1h**, and **1m** samples obtained from **1c** are presented in Fig. S2 and S3. These data are almost identical to our earlier published results^{3,4} confirming independently that the same compounds were obtained. We additionally examined **1a**, **1h**, **1m** samples to check for weak ferromagnetism, similar to that observed in **1c**. However, for **1m** and **1h** there is no difference between zfc and fc curves measured at low field, and the magnetization at 2 K is fully reversible around zero field. For **1m** a small hysteresis loop is observed, but only at the critical field of the metamagnetic transition, so the origin of this effect is different than the weak ferromagnetism. For **1a** zfc/fc curves bifurcate at the transition temperature 4.7 K, but $M(H)$ at 2 K is linear at low fields. No spike at the transition temperature was observed in low-field susceptibility for **1a**, **1h**, **1m**, making **1c** exceptional in this respect.

Conclusions

$\{[\text{Ni}(\text{cyclam})]_3[\text{W}(\text{CN})_8]_2 \cdot \text{solv}\}_n$ (**1c**) augments the family of pseudo-polymorphic supramolecular isomers of the 2D microporous magnetic network $\{[\text{Ni}(\text{cyclam})]_3[\text{W}(\text{CN})_8]_2\}_n$. Together with three earlier obtained forms: solvent-free **1a**, hydrate **1h** and methanol solvate **1m** it constitutes the largest family of structurally and magnetically characterised forms among octacyanometallate-based assemblies. All solvates of the network can be obtained directly from synthesis by applying different conditions. There are several conversion pathways between different forms, both reversible and irreversible, two of which are single-crystal-to-single-crystal transformations. The most stable form is hexadecahydrate, due to the presence of hydrogen bonds stabilizing the network.

All forms are metamagnetic, as can be expected for layered structures, but they significantly differ in magnetic properties. The T_c value increases in the series **1a** < **1h** < **1m** < **1c** from 5 to 12 K, reflecting the straightening of CN-bridges and the resulting stronger intra-layer ferromagnetic interactions. The critical field of metamagnetic transition ranging from 11.5 kOe for **1h** to 1.2 kOe for **1m** is connected with the thickness of the corrugated layers and the distance between them, but is also influenced by H-bond formation between the network and guest molecules.

The pentadecanuclear clusters proved to be an interesting alternative source of $[\text{W}(\text{CN})_8]^{3-}$ ions for the synthesis of more stable, higher dimensionality network. The ions released slowly from the cluster facilitate the growth of the crystalline product.

Acknowledgements

We acknowledge the financial support of the Polish National Science Centre (research grant 2011/01/B/ST5/00716) and the Polish Ministry of Science and Higher Education (Diamond Grant 0195/DIA/2013/42). The research was in part carried out with the equipment purchased with the support of the European Regional Development Fund within the Polish Innovation Economy Operational Program (POIG.02.01.00-12-023/08).

Table 1 Comparison of structural data and magnetic properties for different forms of $\{[\text{Ni}(\text{cyclam})]_3[\text{W}(\text{CN})_8]_2\}_n$: **1a** - anhydrous, **1h** - hydrated, **1m** - MeOH-modified, **1c** - synthesised from Ni_9W_6 cluster (standard uncertainties given in parenthesis where applicable)

	1a	1h	1m	1c
system	triclinic	triclinic	triclinic	monoclinic
space group	P-1	P-1	P-1	C 1 2/m 1
corresponding cell dimensions / Å (periods) and ° (angles)	a = 9.0677(6) b = 15.221(1) c = 15.8788(10) $\alpha = 60.446(5)$ $\beta = 87.419(4)$ $\gamma = 89.916(3)$	a = 8.7270(2) b = 15.2575(4) c = 15.9146(6) $\alpha = 67.406(2)$ $\beta = 87.077(1)$ $\gamma = 87.160(1)$	a = 9.163(2) b = 14.894(5) c = 16.304(5) $\alpha = 73.65(3)$ $\beta = 92.59(3)$ $\gamma = 90.67(3)$	c = 9.331(5) b = 15.068(5) a = 32.105(5) $\gamma = 90$ $\beta = 90.772(5)$ $\alpha = 90$
V/Z / Å ³	1904	1953	2133	2257
bridge angles / °				
Ni2-N-C	157.9(5)	161.0(6)	-	172.3(4)
Ni3-N-C	149.7(4)	159.5(6)	-	172.3(4)
Ni4-N-C	158.1(4)	160.1(7)	-	178.7(8)
intra-layer distances / Å				
W1-Ni2	5.29	5.29	5.39	5.43
W1-Ni3	5.18	5.28	5.40	5.43
W1-Ni4	5.23	5.27	5.35	5.37
layer separation* / Å	7.40	7.38	8.05	8.11
inter-layer distances / Å				
W1-Ni2	7.50	7.32	8.20	8.58
W1-Ni3	7.45	7.75	8.11	8.58
W1-Ni4	8.65	8.45	9.01	8.59
CShM parameters for W**				
TDD-8	1.020	0.976	1.504	2.230
SAPR-8	1.587	1.334	2.686	0.153
angles at W nodes / °				
C11-W1-C13	73.1(2)	73.2(3)		76.1(2)
C11-W1-C16	136.8(2)	136.3(3)		140.57(12)
C16-W1-C13	128.2(2)	128.5(3)		140.57(12)

Ni2-W1-Ni3	92.29	92.37	86.62	87.90
Ni2-W1-Ni4	124.74	122.69	117.34	134.91
Ni3-W1-Ni4	124.62	133.69	146.79	134.91
sum	341.65	348.75	350.75	357.72
layer thickness ^{***} / Å	2.49	1.98	1.65	0.90
mean ring diameter ^{****} / Å	18.84	19.12	19.31	19.70
channel-layer angle / °	54.7	57.5	61.5	60.4
T_c / K	4.9	8.3	11.4	12.0
$(\chi T)_{\max}$ / cm ³ Kmol ⁻¹	5.4	11.6	113	39.3
H_c / kOe	9.0	11.5	1.2	3.2

* layer separation calculated as $d(1\ 0\ -1)$ for **1a**, **1h** and **1m** and $d(2\ 0\ -1)$ for **1c**

** continuous shape measure parameters calculated with SHAPE¹⁹; TDD-8 = trigonal dodecahedron, SAPR-8 = square antiprism

*** thickness of corrugated honeycomb-like layers composed of metal ions and bridging ligands (see Fig. 2) calculated as a displacement of W from the plane defined by Ni ions

**** mean ring diameter calculated as an average distance between opposite metal centres

References

1. S. Kitagawa, R. Kitaura, S. Noro, *Angew. Chem. Int. Ed.*, 2004, **43**, 2334–2375; P. Dechambenoit, J. R. Long, *Chem. Soc. Rev.*, 2011, **40**, 3249–3265.
2. E. Coronado, G. Minguez-Espallargas, *Chem. Soc. Rev.*, 2013, **42**, 1525–1539.
3. B. Nowicka, M. Rams, K. Stadnicka and B. Sieklucka, *Inorg. Chem.*, 2007, **46**, 8123–8125.
4. B. Nowicka, M. Bałanda, B. Gawel, G. Ćwiak, A. Budziak, W. Łasocha and B. Sieklucka, *Dalton Trans.*, 2011, **40**, 3067–3073.
5. B. Nowicka, M. Bałanda, M. Reczyński, A. M. Majcher, M. Koziel, W. Nitek, W. Łasocha and B. Sieklucka, *Dalton Trans.*, 2013, **42**, 2616–2621.
6. F. Bonadio, M. Gross, H. Stoeckli-Evans and S. Decurtins, *Inorg. Chem.* 2002, **41**, 5891–5896.
7. M. G. Hilfiger, H. Zhao, A. Prosvirin, W. Wernsdorfer and K. R. Dunbar, *Dalton Trans.* 2009, 5155–5163; J. H. Lim, H. S. Yoo, J. I. Kim, J. H. Yoon, N. Yang, E. K. Koh, J.-G. Park and C. S. Hong, *Eur. J. Inorg. Chem.*, 2008, 3428–3431; J. H. Lim, H. S. Yoo, Y. H. Yoon, E. K. Koh, H. C. Kim and C. S. Hong, *Polyhedron*, 2008, **27**,

- 299–303; J. H. Lim, Y. H. Yoon, H. C. Kim, and C. S. Hong, *Angew. Chem. Int. Ed.*, 2006, **45**, 7424–7426.
8. Z. J. Zhong, H. Seino, Y. Mizobe, M. Hidai, A. Fujishima, S. Ohkoshi and K. Hashimoto, *J. Am. Chem. Soc.* 2000, **122**, 2952–2953; Y. Song, P. Zhang, X.-M. Ren, X.-F. Shen, Y.-Z. Li and X.-Z. You, *J. Am. Chem. Soc.* 2005, **127**, 3708–3709.
9. R. Podgajny, W. Nitek, M. Rams and B. Sieklucka, *Cryst. Growth Des.*, 2008, **8**, 3817–3821; R. Podgajny, S. Chorąży, W. Nitek, M. Rams, M. Bałanda and B. Sieklucka, *Cryst. Growth Des.*, 2010, **10**, 4693–4696; S. Chorąży, R. Podgajny, W. Nitek, M. Rams, S. Ohkoshi, B. Sieklucka; *Cryst. Growth Des.*, 2013, **13**, 3036–3045.
10. D. E. Berry, S. Girard and A. McAuley; *J. Chem. Edu.*, 1996, **73**, 551–554.
11. C. R. Dennis, A. J. van Wyk, S. S. Basson and J. G. Leipoldt; *Transition Met. Chem.*, 1992, **17**, 471–473.
12. A. Altomare, M. C. Burla, M. Camalli, G. L. Cascarano, C. Giacovazzo, A. Guagliardi, A. G. G. Moliterni, G. Polidori and R. Spagna, *J. Appl. Cryst.*, 1999, **32**, 115–119.
13. Agilent: *CrysAlis PRO*, Agilent Technologies UK Ltd, Yarnton, England, 2011.
14. A. L. Spek, *Acta Cryst. D*, 2009, **65**, 148–155.
15. G. M. Sheldrick, *Acta Crystallogr. A.*, 2008, **64**, 112–122.
16. C. F. Macrae, P. R. Edgington, P. McCabe, E. Pidcock, G. P. Shields, R. Taylor, M. Towler and J. van de Streek; *J. Appl. Crystallogr.*, 2006, **39**, 453–457.
17. S. R. Batten, S. M. Neville, D. R. Turner *Coordination Polymers: Design, Analysis and Application*; RSC Publishing, Cambridge, United Kingdom, 2009.
18. B. Nowicka, T. Korzeniak, O. Stefańczyk, D. Pinkowicz, S. Chorąży, R. Podgajny and B. Sieklucka, *Coord. Chem. Rev.*, 2012, **256**, 1946–1971.
19. M. Llunell, D. Casanova, J. Cirera, P. Alemany, S. Alvarez: *SHAPE v. 2.1*, University of Barcelona, Barcelona, Spain, 2013.
20. R. Lescouezec, J. Vaissermann, C. Ruiz-Perez, F. Lloret, R. Carrasco, M. Julve, M. Verdaguer, Y. Dromzee, D. Gatteschi, and W. Wernsdorfer, *Angew. Chem. Int. Ed.* 2003, **42**, 1483 – 1486; C. Mukherjee, V. Hoeke, A. Stammler, H. Bögge, J. Schnack and T. Glaser, *Dalton Trans.* 2014, **43**, 9690–9703; T. D. Harris, C. Coulon, R. Clerac and J. R. Long, *J. Am. Chem. Soc.* 2011, **133**, 123–130.
21. T. Moriya, *Phys. Rev.*, 1960, **120**, 91.
22. R. L. Carlin, *Magnetochemistry*, Springer, 1986.

Figures

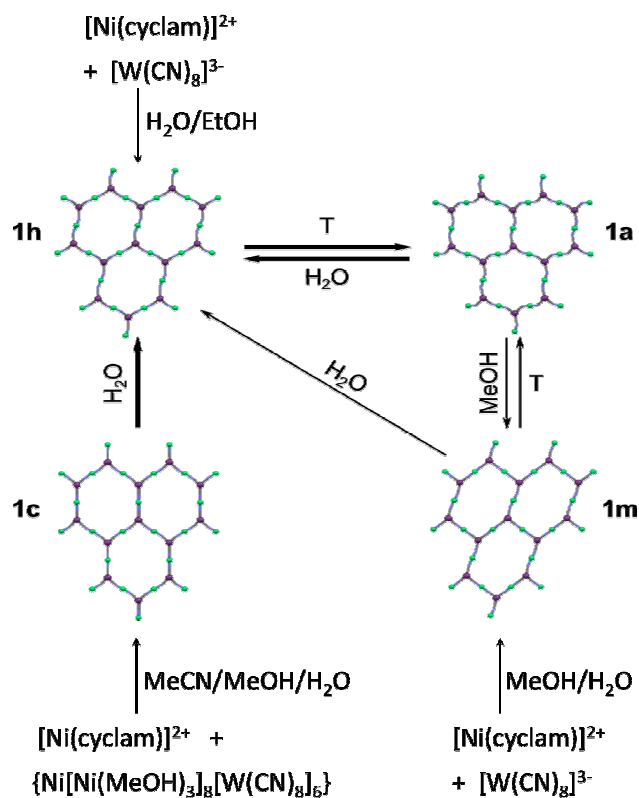


Fig. 1. Synthetic routes and structural transformation pathways of $\{[\text{Ni}(\text{cyclam})]_3[\text{W}(\text{CN})_8]_2\}_n$ (1). View parallel to the channels; only metal ions (Ni - green, W - purple balls) and bridging CN ligands (C - grey, N - blue sticks) presented for clarity. Bold arrows mark single-crystal-to-single-crystal transformations.

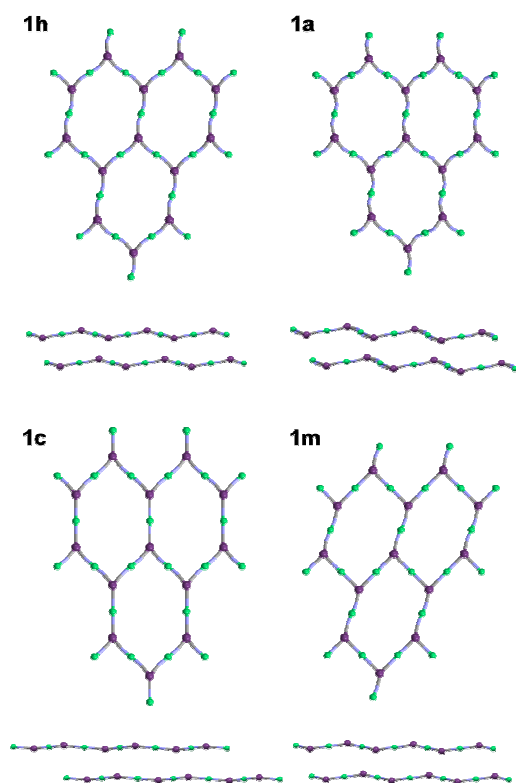


Fig. 2. Different structural forms of **1**. View perpendicular to layer (top), and parallel to the layers (bottom). Only metal ions and bridging CN ligands presented for clarity (colours like in Fig. 1).

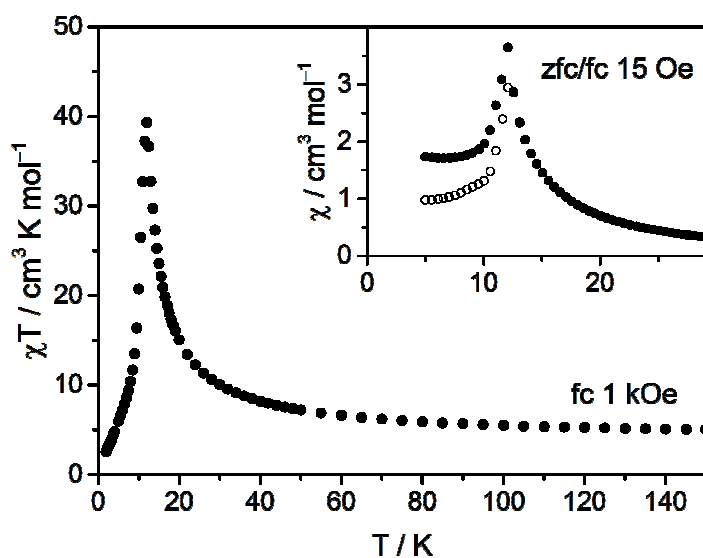


Fig. 3. Temperature dependence of magnetic susceptibility of **1c** measured at 1 kOe. Inset: Zero-field cooled (empty circles) and field cooled (full circles) susceptibility measured with 0.5 K spacing at low field.

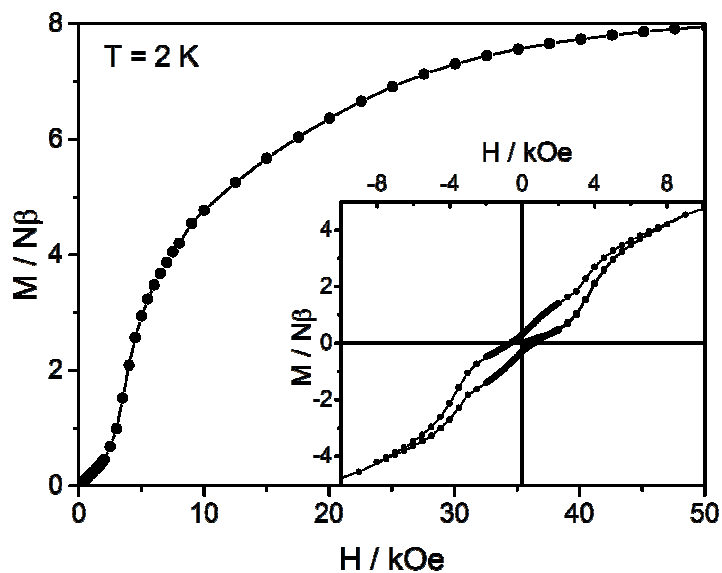


Fig. 4. Magnetization vs. field plot for **1c** at 2 K; inset: hysteresis loop measured at 2 K in the range from -10 to 10 kOe.

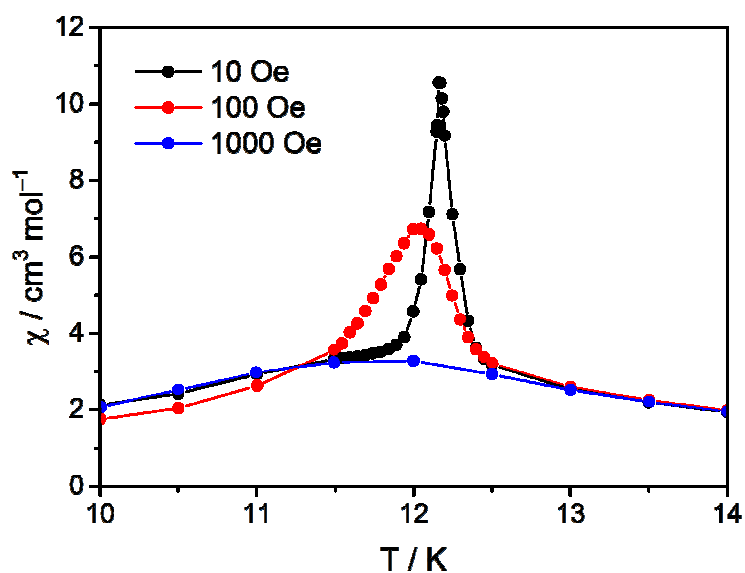


Fig. 5. Temperature dependence of magnetic susceptibility measured for **1c** at different applied fields with small temperature spacing.

Larger pores and higher T_c : $\{[\text{Ni}(\text{cyclam})]_3[\text{W}(\text{CN})_8]_2 \cdot \text{solv}\}_n$ - a new member of the largest family of pseudo-polymorphic isomers among octacyanomethylate-based assemblies

Beata Nowicka,^{*a} Mateusz Reczyński,^a Michał Rams,^b Wojciech Nitek,^a Marcin Koziel,^a and Barbara Sieklucka^a

^a*Faculty of Chemistry, Jagiellonian University, Ingardena 3, 30-060 Kraków, Poland*

^b*Institute of Physics, Jagiellonian University, Łojasiewicza 11, 30-348 Kraków, Poland*

Graphical abstract

New form of 2D honeycomb-like network is characterised by flat layers and undergoes single-crystal-to-single-crystal transformation to corrugated hexadecahydrate.

